2021 IEEE 12th International Symposium on Power Electronics for Distributed Generation Systems (PEDG) | 978-1-6654-0465-5/21/$31.00 ©2021 IEEE | DOI: 10.1109/PEDG51384.2021.9494173

Sliding Mode Control Scheme of a Cascaded H-Bridge Multilevel Active Front End Rectifier

Garry Jean-Pierre[1], Necmi Altin[2], and Adel Nasiri[1]
[1] Center for Sustainable Electrical Energy Systems, University of Wisconsin-Milwaukee (UWM)
[2] Department of Electrical & Electronics Engineering, Faculty of Technology, Gazi University, Ankara, Turkey
jeanpie4@uwm.edu, naltin@gazi.edu.tr, nasiri@uwm.edu

***Abstract*—In this study, a sliding mode control (SMC) scheme is proposed for the single-phase cascaded H-bridge (CHB) multilevel active front end (AFE) rectifier with LCL filter. A PI controller is employed to control the DC voltage of the rectifier modules and to obtain the amplitude for the reference grid current. The SMC based current control scheme uses the grid current and filter capacitor voltage feedbacks. The resonance of the LCL filter is damped using the voltage feedback of the capacitor. Therefore, the requirement for additional damping circuitry is removed. Simulation and experimental results are presented to verify the performance of the SMC for the CHB multilevel AFE rectifier. The overall proposed control scheme provides almost unity power factor and fast transient response. It is seen from the results that the current drawn from the grid is in sinusoidal waveform with low THD.**

Keywords — cascaded H-bridge, sliding mode controller, active front end, resonance damping

I. INTRODUCTION

Innovation in power electronics made it possible to operate at voltage levels far off the conventional semiconductor operating limits. New multilevel converter configurations have been studied for medium and high voltage applications. These converters are able to achieve high voltage switching through different voltage steps. The multilevel converter topologies can be classified into three main groups: flying capacitor, neutral point clamped, and cascaded H-bridge (CHB) converters. CHB is a promising configuration for medium and high power applications. It presents numerous advantages, such as the ability to provide better harmonic attenuation and mitigate electromagnetic interference. Additionally, it can be configured by cascading multiple single-phase H-bridge modules into one compact system. This structure can provide a low cost solution for the medium-voltage high-power conversion applications due to requiring a smaller number of switching devices and components than other multilevel converter topologies with the same voltage rating [1]-[2].

When configured as a rectifier, the CHB converter has multiple DC-link voltages which can be used for different power ratings, making this topology an excellent choice for traction applications, solid state transformers, and medium and high power motor drives [3]-[5]. However, this configuration comes with some drawbacks: isolated power supplies become a requirement when the converter is operating as a voltage source inverter and achieving unity power factor while operating at the desired limits of the device can be cumbersome [6]-[7].

A DC-side voltage control, the grid voltage synchronization, and the grid current control are the typical components of a CHB AFE rectifier control unit. A 3-D space modulation scheme was presented in [8] to achieve DC voltage balancing in all operation modes. A hybrid modulation technique was presented in [9] for both balancing DC voltage using the low-frequency switching and for grid current control utilizing the high-frequency sinusoidal pulse width modulation. In [10], a cascaded PI controller was used to regulate both the DC voltage and the utility current. The model predictive control was utilized in [11] for fault localization and in [12] to reduce high computational complexity and to improve the steady-state performance of the current. In [13], a dual-model predictive control technique was presented to enhance the dynamic and harmonic performance and to balance the DC voltage.

The control strategies employed in CHB AFE rectifiers are used to achieve the following objectives: produce constant output DC-link voltage, draw sinusoidal grid current, and balance the DC bus voltage of the capacitor. In addition to the different control methods used in [7]-[12], nonlinear control was used in [14], where a modified Lyapunov control strategy combined with a proportional resonant controller and a voltage balancing controller was studied to control the CHB rectifier.

In regards to the current control strategy, numerous current-tracking techniques have been presented. A small signal decoupled *dq* current control method [15] was used to solve the issue of low frequency oscillation. The hysteresis and discrete pulse current control techniques were presented in [16] to realize same switching frequencies between the inverter switches. A proportional resonant current regulation method was studied in [17] to maintain the grid current in sinusoidal and to achieve low THD. The model predictive current control method was studied and compared to other traditional current control techniques in [18] to establish its simplicity and operating principles. A transient current control method based notch filter approach was studied in [19] to eliminate the oscillation in rail road power electronic applications.

The SMC, a well-known nonlinear control method, has been studied in many converter topologies. It was used in a neutral-point clamped converter to improve steady-state and dynamic performance [20]. The SMC presented in [21] was used for a 7-level grid-tied inverter. Through manipulation of the hysteresis bandwidth of the error resulting from the capacitor voltage control, the minimum average switching frequency was obtained. A variant of the SMC was studied in [22] in a three-

978-1-6654-0465-5/21/$31.00 ©2021 IEEE

phase grid-connected system for wind energy to control the reactive and active power flows between the system and the grid. In [23] and [24], SMC was presented to control the single-phase and three-phase grid connected inverters with LCL filters and no additional active or passive resonance damping methods. A space vector modulation based SMC was studied in [25] to regulate the grid current and the flow of active and reactive power in a three-level grid-connected neutral point clamped inverter. SMC technique was proposed in [26] to eliminate error in the grid current tracking accuracy and to decrease the THD of a single-phase grid-connected voltage source inverter with an LCL filter. In addition, the SMC was proposed to control the current of grid-connected two-leg reduced number of switch neutral point clamped and T-type multilevel inverters [27] and [28].

Due to the excellent features of the SMC, such as tracking grid current, drawing current with reduced harmonic components, and controlling the output voltage and reactive and active power for various converter topologies, this paper studies the SMC based current control scheme for the single-phase CHB AFE rectifier. The proposed control scheme employs a PI DC voltage controller and a high performance current control scheme based on the SMC. The proposed system is validated with simulation and experimental results. The results show that the proposed system is drawing sinusoidal currents which are in the same phase with the grid voltage and at the same frequency, even for low load conditions. In addition, the proposed system is tested for step load changes and it is seen that the control method offers fast dynamic response and removes the steady-state error.

II. Modeling of the CHB Multilevel AFE

The CHB multilevel rectifier circuits have the same advantages of the multilevel converters. The CHB is inherently in modular structure and can be considered as a serial connection of number of H-bridges. With this feature, this topology is very suitable to handle high voltage levels, and enables direct medium voltage connection. Along with these advantages, each H-bridge in this topology generates an output DC voltage.

In high power isolated DC-DC converter applications, due to the high frequency magnetic material core size limitations, it is very common to use parallel connected multiple isolated dc-DC converter units. If the primary side of the system is at high voltage level, this high voltage side can be connected in series to handle the high voltage level, while the low voltage secondary windings can be connected in parallel. This topology is called input series output parallel topology and it is very attractive high power high frequency medium voltage to low voltage applications. With multiple output voltage generation capability, the CHB is naturally generated the required input voltages for the isolated DC-DC converter units. Thus primary side voltage levels can be divided into the number of converter units. The output of the converter units can be connected in parallel to obtain the same power capability with input series output parallel topology.

A single-phase CHB multilevel AFE rectifier output is shown in Fig. 1. It is composed of three identical single-phase H-bridge modules generating three separate DC bus voltages, V_{o1}, V_{o2} and V_{o3}. An LCL filter is installed to filter out the high frequency components from the current drawn from the grid. The LCL filter is composed of Z_1, Z_2 and C_f . Here, Z_2 is the series combination of L_2 and r_2. Z_1 is the series combination of L_1 and r_1. The equations describing the CHB converter can be written as (1) – (6).

$$L_2 \frac{di_2}{dt} + r_2 i_2 = v_g - v_{c_f} \tag{1}$$

$$L_1 \frac{di_1}{dt} + r_1 i_1 = v_{c_f} - (V_{H_1} + V_{H_2} + V_{H_3}) \tag{2}$$

$$C_f \frac{dv_{c_f}}{dt} = i_c = i_2 - i_1 \tag{3}$$

$$V_{H_1} = uV_{o_1},\ V_{H_2} = uV_{o_2},\ V_{H_3} = uV_{o_3} \tag{4}$$

$$V_{0_1} = V_{0_2} = V_{0_3} = V_d \tag{5}$$

$$v_g = V_g \sin(wt) \tag{6}$$

Equation (7) represents the switching function in which U_o is defined as the steady-state value of u and Δu as the perturbed component of u.

$$u = U_0 + \Delta u \tag{7}$$

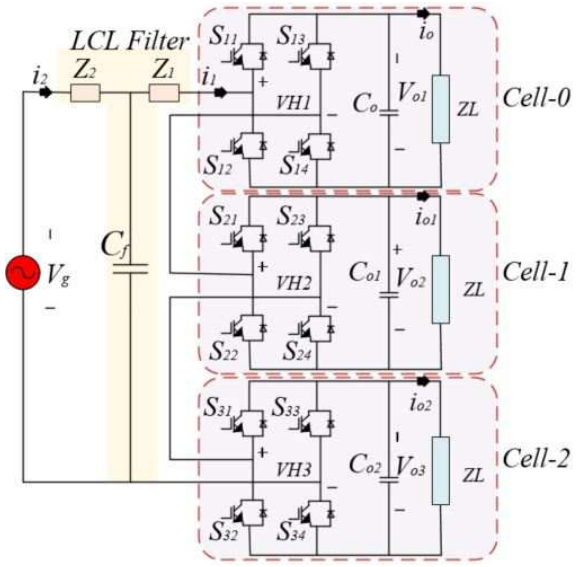

Fig. 1. The CHB multilevel active front end rectifier circuit.

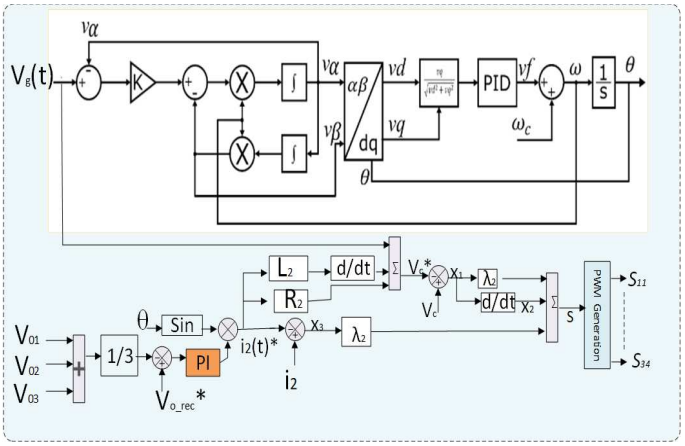

Fig. 2. The overall control structure of the system.

III. Proposed Control Scheme

Fig. 2 shows the proposed control scheme for the control of the CHB multilevel AFE rectifier. The PI method is used to regulate the output DC voltage. The number of output voltages, *n,* is summed and divided by *n.* In this case, *n* = 3. This value is controlled to track the desired voltage value. The PI controller generates the amplitude of the reference current value. By using the PLL output, the reference current signal for the current controller is generated.

The state-variables can be formulated in (7) – (9), where i_1^*, i_2^* and v_{cf}^* are the references for i_1, i_2 and v_{cf}.

$$x_1 = v_{C_f} - v_{C_f}^* \tag{8}$$

$$x_2 = \dot{v}_{C_f} - \dot{v}_{C_f}^* \tag{9}$$

$$x_3 = i_2 - i_2^* \tag{10}$$

The reference signal of the grid current is defined by the DC voltage controller. A PI controller is employed to track the DC voltage reference (V_o*), as given below:

$$I_2^* = K_P(V_0^* - V_o) + K_I \int (V_0^* - V_o)dt \tag{11}$$

$$i_2^* = I_2^* sin\omega t \tag{12}$$

where $sin\omega t$ is obtained from the PLL. i_1^* and v_{cf}^* can be obtained, as below:

$$i_1^* = i_2^* - i_{C_f}^* \tag{13}$$

$$v_{C_f}^* = v_g - L_2 \frac{di_2^*}{dt} - r_2 i_2^* \tag{14}$$

A- SMC Control Scheme

The sliding surface is defined as

$$S = \lambda_1 x_1 + x_2 + \lambda_2 x_3 \tag{15}$$

where λ_1 and λ_2 are positive real constants. When the system enters into the sliding mode ($S = 0$), the state variables are forced to move on a sliding surface towards the origin ($x_1 = 0$, $x_2 = 0$, and $x_3 = 0$). To ensure that the motion of the state variables is maintained on the sliding surface, the existence condition must be met:

$$S\dot{S} < 0 \tag{16}$$

where $\dot{S}$ represents the time derivative of *S*, and can be written as (17).

$$\dot{S} = \lambda_1 \dot{x}_1 + \dot{x}_2 + \lambda_2 \dot{x}_3 \tag{17}$$

Time derivatives of the state variables can be written as follows:

$$\dot{x}_1 = x_2 \tag{18}$$

$$\dot{x}_2 = 3\omega_1^2 u V_d x_2 - (\omega_1^2 - \omega_2^2)x_1 + A(t) \tag{19}$$

$$\dot{x}_3 = C_f \omega_2^2 \left(x_1 + v_{C_f}^* - v_g\right) - \frac{di_2^*}{dt} \tag{20}$$

where $\omega_1 = 1/\sqrt{L_1 C_f}$, $\omega_2 = 1/\sqrt{L_2 C_f}$, and the disturbance term $A(t)$ is given with

$$A(t) = -(\omega_1^2 - \omega_2^2)v_{C_f}^* - \frac{d^2 v_{C_f}^*}{dt^2} + \omega_2^2 v_g \tag{21}$$

Substituting (18)-(20) into (17) results in

$$\dot{S} = -\left[\omega_1^2 + \left(1 - \lambda_2 C_f\right)\omega_2^2\right]x_1 + \lambda_1 x_2 + 3\omega_1^2 u V_d + B(t) \tag{22}$$

where $B(t)$ is the disturbance term given with:

$$B(t) = -\left[\omega_1^2 - \left(1 - \lambda_2 C_f\right)\omega_2^2\right]v_{C_f}^* + \left(1 - \lambda_2 C_f\right)\omega_2^2 v_g - -\frac{d^2 v_{C_f}^*}{dt^2} - \frac{di_2^*}{dt} \tag{23}$$

To ensure the stability of the control system, existence of the sliding mode operation should be verified by satisfying $S\dot{S} < 0$. The control variable *u* is expressed as below:

$$u = -sign(S) \tag{24}$$

Details on the controller design can be found in [23].

IV. Simulation and Experimental Results

The proposed system is verified with simulation and experimental studies. The proposed controller was studied for both steady-state and transient conditions. For the simulation studies, the following parameters are used: grid voltage is 230V; the inverter side filter inductance is 0.8mH; the grid side filter inductance is 0.5mH; the filter capacitor is 10μF; resistances of inverter and grid side inductors are 0.08Ω and 0.05Ω, respectively; and the DC bus voltage is 200V. The results of the simulation are presented in Fig. 3 – 6.

Fig. 3 and 4 show the steady-state operation of the converter. It is clear in Fig. 3 that the converter draws sinusoidal current from the grid and the current is in phase with the grid voltage. The three DC bus voltages are shown in Fig. 4, which demonstrates the DC voltage tracking accuracy, low overshoot and undershoot, and low capacitor voltage ripple.

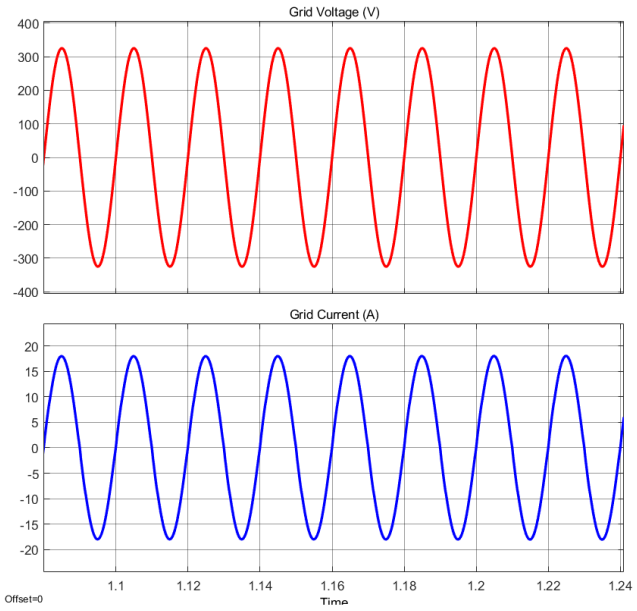

Fig. 3. The grid voltage and current waveforms.

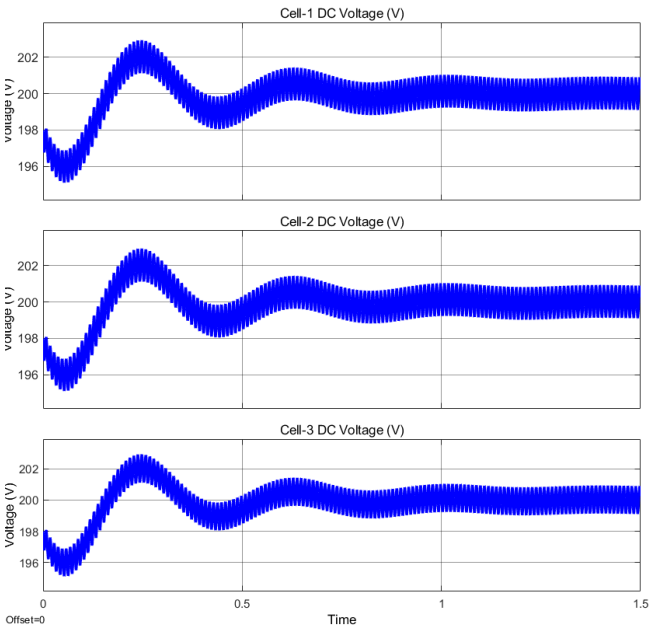

Fig. 4. The DC bus voltages.

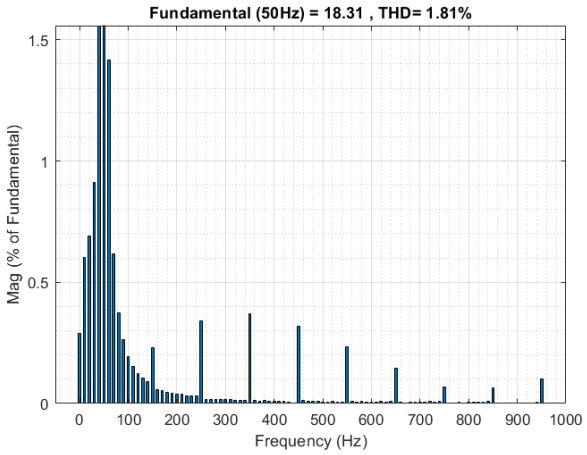

Fig. 5. The harmonic spectrum and THD of the grid current.

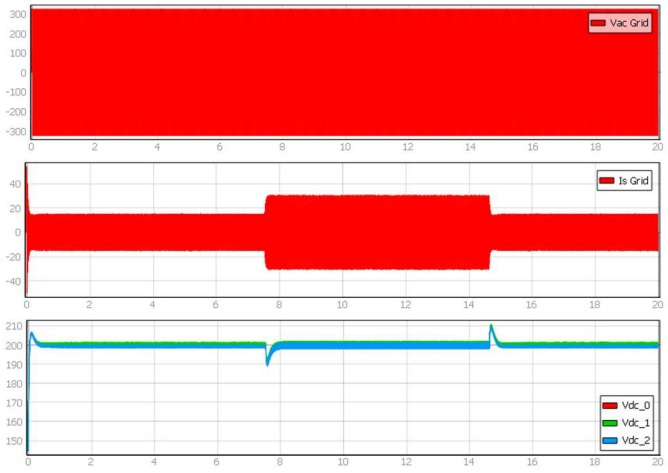

Fig. 6. The grid voltage and current and the DC bus voltages during load step up and down.

It ıs also seen that three output voltages are balanced. The harmonic content of the grid current is also investigated. Fig. 5 shows the current harmonic spectra. It is evident that the proposed SMC based controller provides low grid current THD (1.81%)ö and almost unity power factor is achıeved with synchronized and low harmonıc content grid current.

The experimental results are shown in Fig. 6 – 12. The grid voltage, the grid current and three output DC cell voltages are given in Fig. 6. The dynamic performance of the system was evaluated for both load step up and step down. It is shown that the converter maintains good transient performance and there is no disturbance in the grid current. The overshoot and undershoot during load steps in the DC bus voltages are approximately 5%. The overall strategy provides fast recovery during transients.

The output DC voltage (Ch. 3), the grid voltage (Ch. 1), and current (Ch. 2) waveforms are given in Fig. 7. It is seen that the current drawn from the grid is in sinusoidal waveform and in phase with the grid voltage. The harmonics content of the current signal is low. Besides, the DC output voltages also track their references. Fig. 8 shows the three output DC bus voltages.

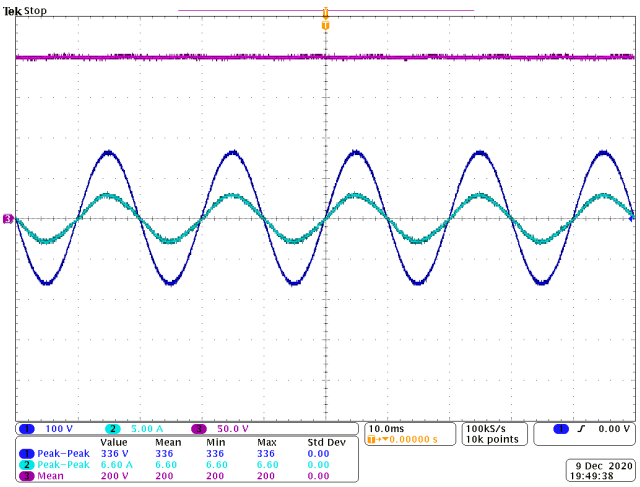

Fig. 7. The grid voltage and current and DC bus voltage of one module.

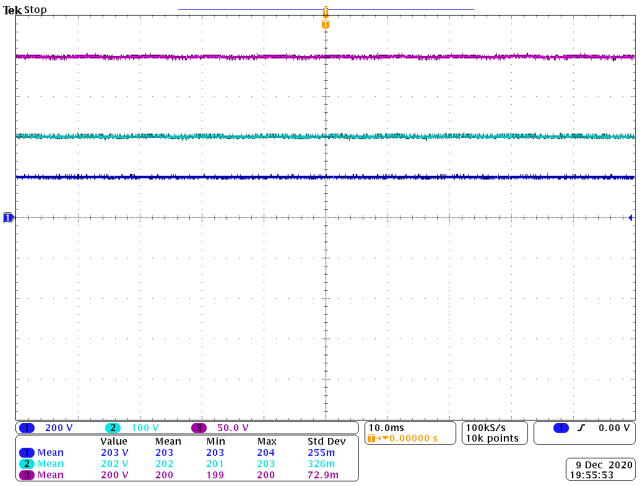

Fig. 8. DC bus voltage of all three modules.

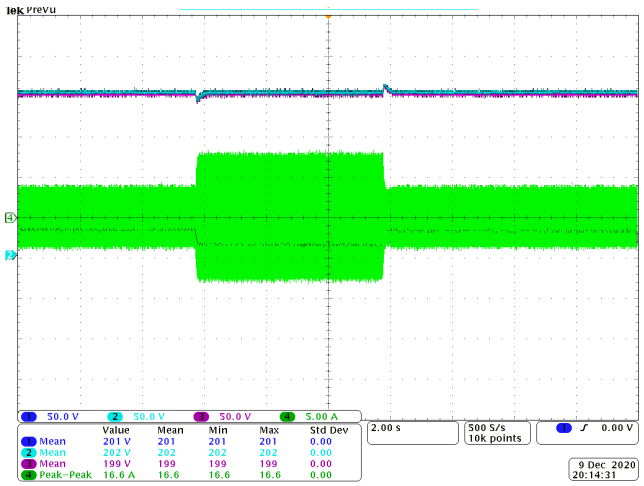

Fig. 9. The grid current and DC bus voltage at load step up and down.

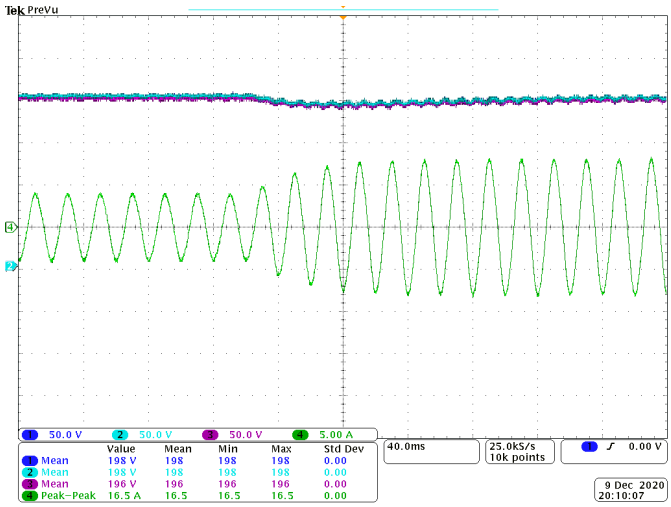

Fig. 10. The grid current and DC bus voltages at load step up.

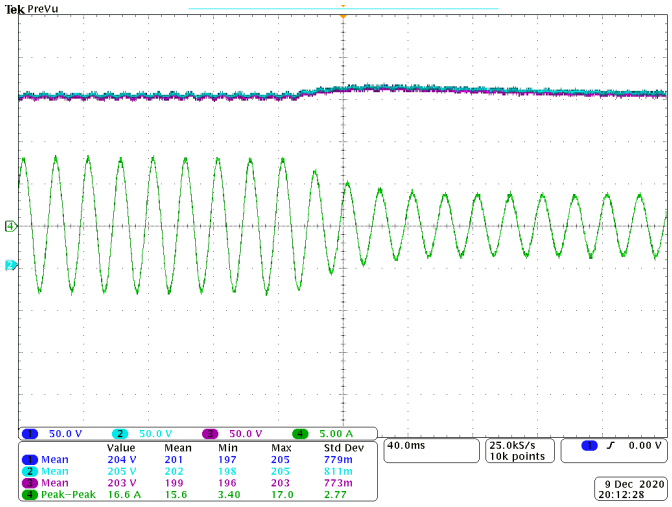

Fig. 11. The grid current and DC bus voltages at load step down.

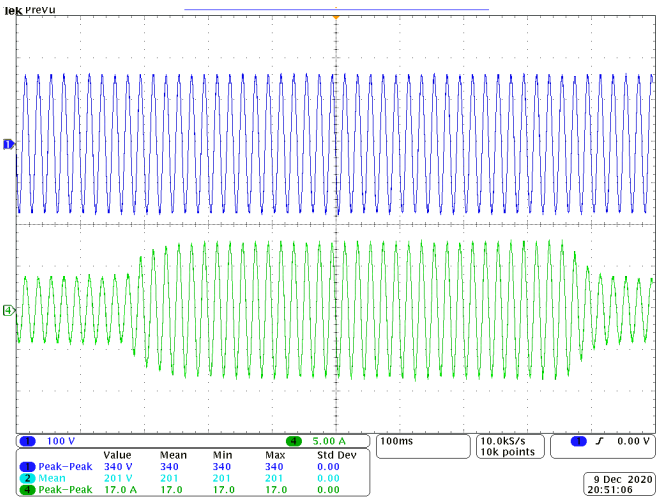

Fig. 12. The grid voltage and current during both load step up and down.

It is seen that all three DC bus voltages are balanced. The transient response of the proposed controller is also tested with experimental studies for a 50% step change in load, from 50% load to 100% load and vice versa, as seen in Fig. 9. The grid current and output DC voltage waveforms are also given in this figure. It is seen that both the DC voltage controller and the sliding mode based current controller yield excellent transient response with low overshoot and undershoot.

In Fig. 10 and 11, the DC voltages of each module and grid current are zoomed in at the transition of the step load to provide better observation of the dynamic performance of the controller. It is clear that the grid current is in sinusoidal waveform even during the transients, and synchronous with the grid phase and frequency. Thus, it is evident that unity power factor is achieved. In addition, the proposed control approach provides fast transient response and suppress the oscillations on the output DC voltage and the grid current. Moreover, the LCL filter resonnat is also suppressed with proposed current controller. The system can offers robust performance. The grid voltage and current are given at the step change instants in Fig. 12.

V. Conclusion

In this study, the SMC scheme has been applied to a single-phase CHB multılevel AFE rectifier. A PI controller was used to control the voltage and generate the amplitude of the current reference signal. By using the PLL system, the grid current reference, which is tracked by the SMC controller, is obtained. The grid current and capacitor voltage of the LCL filter are used as feedback signals. The proposed controller was validated through simulation and the presented experimental results. The simulation and experimental results show that the rectifier current drawn from the grid is in phase with the grid voltage, is in sinusoidal waveform, and has a THD level of 1.81%. Additionally, the resonance of the LCL filter is also damped without any additional active and passive damping methods. This CHM multilevel AFE rectifier with multiple output DC voltages is a suitable topology for high power direct medium voltage connected solid-state transformer applications,

especially when secondary side of the multiple transformer units are connected in parallel to achieve desired power.

ACKNOWLEDGMENT

This material is based upon work supported by the National Science Foundation under Grant No. 1650470. Any opinions, findings, and conclusions or recommendations expressed in this material are those of the author(s) and do not necessarily reflect the views of the National Science Foundation.

REFERENCES

[1]- J. Wen and K. Ma Smedley, "Synthesis of Multilevel Converters Based on Single- and/or Three-Phase Converter Building Blocks," *IEEE Transactions on Power Electronics*, vol. 23, no. 3, pp. 1247-1256, May 2008.

[2]- N. B. Kadandani, S. Ethni, M. Dahidah and H. Khalfalla, "Modelling, Design and Control of Cascaded H-Bridge Single Phase Rectifier,"*2019 10th International Renewable Energy Congress (IREC)*, Sousse, Tunisia, 2019, pp. 1-6.

[3]- J. Rodriguez, S. Bernet, B. Wu, and J. O. Pontt, "Multilevel voltage source converter topologies for industrial medium voltage drives," IEEE Trans. Ind. Electron., vol. 54, no. 6, pp. 2930–2945, Dec.

[4]- B. Han, B. Bae, S. Baek, and G. Jang, "New configuration of UPQC for medium-voltage application," IEEE Trans. Power Delivery, vol. 21, no. 3, pp. 1438–1444, Jul. 2006.

[5]- A. M. Massoud, S. J. Finney, A. J. Cruden, and B. W. Williams, "Threephase, three-wire, five-level cascaded shunt active filter for power conditioning, using two different space vector modulation techniques," IEEE Trans. Power Delivery, vol. 22, no. 4, pp. 2349–2361, Oct. 2007.

[6]- S. Vazquez, J. I. Leon, J. M. Carrasco, L. G. Franquelo, E. Galvan, M. Reyes, J. A. Sanchez, and E. Dominguez, "Analysis of the power balance in the cells of a multilevel cascaded H-bridge converter," IEEE Trans. Ind. Electron., vol. 57, no. 7, pp. 2287–2296, Jul. 2010.

[7]- A. S. Gadalla, X. Yan and H. Hasabelrasul, "Active Power Analysis for the Battery Energy Storage Systems Based on a Modern Cascaded Multilevel Converter,"*2018 IEEE International Conference on Energy Internet (ICEI)*, Beijing, 2018, pp. 111-116.

[8]- X. She, A. Q. Huang and G. Wang, "3-D Space Modulation with Voltage Balancing Capability for a Cascaded Seven-Level Converter in a Solid-State Transformer," in IEEE Transactions on Power Electronics, vol. 26, no. 12, pp. 3778-3789, Dec. 2011.

[9]- M. Moosavi, G. Farivar, H. Iman-Eini and S. M. Shekarabi, "A voltage balancing strategy with extended operating region for cascaded H-bridge converters," in IEEE Transactions on Power Electronics, vol. 29, no. 9, pp. 5044-5053, Sept. 2014.

[10]- Cecati, A. Dell'Aquila, M. Liserre and V. G. Monopoli, "Design of H-bridge multilevel active rectifier for traction systems," *IEEE Transactions on Industry Applications*, vol. 39, no. 5, pp. 1541-1550, Sept.-Oct. 2003.

[11]- L. Tarisciotti, P. Zanchetta, A. Watson, P. Wheeler, J. C. Clare and S. Bifaretti, "Multiobjective Modulated Model Predictive Control for a Multilevel Solid-State Transformer," in IEEE Transactions on Industry Applications, vol. 51, no. 5, pp. 4051-4060, Sept.-Oct. 2015.

[12]- C. Qi, X. Chen, P. Tu and P. Wang, "Cell-by-Cell-Based Finite-Control-Set Model Predictive Control for a Single-Phase Cascaded H-Bridge Rectifier," *IEEE Transactions on Power Electronics*, vol. 33, no. 2, pp. 1654-1665, Feb. 2018.

[13]- M. Chai, N. B. Y. Gorla and S. K. Panda, "Improved Performance with Dual-Model Predictive Control for Cascaded H-Bridge Multilevel Converter," in IEEE Transactions on Industry Applications, vol. 55, no. 5, pp. 4886-4899, Sept.-Oct. 2019.

[14]- G. Jean-Pierre, N. Altin, A. E. Shafei and A. Nasiri, "A Control Scheme Based on Lyapunov Function for Cascaded H-Bridge Multilevel Active Rectifiers," 2020 IEEE Applied Power Electronics Conference and Exposition (APEC), New Orleans, LA, USA, 2020, pp. 2021-2026.

[15]- K. Jiang, C. Zhang, and X. Ge, "Low-frequency oscillation analysis of the train-grid system based on an improved forbidden-region criterion," IEEE Trans. Ind. Appl., vol. 54, no. 5, pp. 5064–5073, Sep./Oct. 2018.

[16]- P. A. Dahono, "New hysteresis current controller for single-phase full bridge inverter," IET Power Electron., vol. 2, no. 5, pp. 585–594, Sep. 2009.

[17]- D. Dujic et al., "Power electronic traction transformer-low voltage prototype," IEEE Trans. Power Electron., vol. 28, no. 12, pp. 5522–5534, Dec. 2013.

[18]- S. Kouro, P. Cortes, R. Vargas, U. Ammann, and J. Rodriguez, "Model predictive control—A simple and powerful method to control power converters," IEEE Trans. Ind. Electron., vol. 56, no. 6, pp. 1826–1838, Jun. 2009

[19]- Z. Shuai, H. Cheng, J. Xu, C. Shen, Y. Hong, and Y. Li, "A notch filter based active damping control method for low frequency oscillation suppression in train-network interaction systems," IEEE J. Emerg. Sel. Topics. Power Electron., vol. 7, no. 4, pp. 2417–2427, Dec. 2019.

[20]- X. Shen et al., "High-Performance Second-Order Sliding Mode Control for NPC Converters," in IEEE Transactions on Industrial Informatics, vol. 16, no. 8, pp. 5345-5356, Aug. 2020.

[21]- H. Makhamreh, M. Trabelsi, O. Kükrer and H. Abu-Rub, "An Effective Sliding Mode Control Design for a Grid-Connected PUC7 Multilevel Inverter," in IEEE Transactions on Industrial Electronics, vol. 67, no. 5, pp. 3717-3725, May 2020.

[22]- X. Zheng, Y. Feng, F. Han and X. Yu, "Integral-Type Terminal Sliding-Mode Control for Grid-Side Converter in Wind Energy Conversion Systems," in IEEE Transactions on Industrial Electronics, vol. 66, no. 5, pp. 3702-3711, May 2019.

[23]- H. Komurcugil, S. Ozdemir, I. Sefa, N. Altin and O. Kukrer, "Sliding-Mode Control for Single-Phase Grid-Connected LCL-Filtered VSI With Double-Band Hysteresis Scheme," in IEEE Transactions on Industrial Electronics, vol. 63, no. 2, pp. 864-873, Feb. 2016.

[24]- N. Altin, S. Ozdemir, H. Komurcugil and I. Sefa, "Sliding-Mode Control in Natural Frame With Reduced Number of Sensors for Three-Phase Grid-Tied LCL-Interfaced Inverters," in IEEE Transactions on Industrial Electronics, vol. 66, no. 4, pp. 2903-2913, April 2019.

[25]- F. Sebaaly, H. Vahedi, H. Y. Kanaan, N. Moubayed and K. Al-Haddad, "Design and Implementation of Space Vector Modulation-Based Sliding Mode Control for Grid-Connected 3L-NPC Inverter," in IEEE Transactions on Industrial Electronics, vol. 63, no. 12, pp. 7854-7863, Dec. 2016.

[26]- X. Hao, X. Yang, T. Liu, L. Huang and W. Chen, "A Sliding-Mode Controller with Multiresonant Sliding Surface for Single-Phase Grid-Connected VSI With an LCL Filter," in IEEE Transactions on Power Electronics, vol. 28, no. 5, pp. 2259-2268, May 2013.

[27]- S. Ozdemir, N. Altin, H. Komurcugil and I. Sefa, "Sliding Mode Control of Three-Phase Three-Level Two-Leg NPC Inverter with LCL Filter for Distributed Generation Systems," IECON 2018 - 44th Annual Conference of the IEEE Industrial Electronics Society, 2018, pp. 3895-3900.

[28]- N. Altin, S. Ozdemir, H. Komurcugil, I. Sefa and S. Biricik, "Sliding-Mode and Proportional-Resonant Based Control Strategy for Three-Phase Two-Leg T - Type Grid-Connected Inverters with LCL Filter," IECON 2018 - 44th Annual Conference of the IEEE Industrial Electronics Society, 2018, pp. 4492-4497.